reduction temperatures in the range 673-773 K (curve a), a significant decrease of I_A is observed; this variation corresponds to the elimination of previously incorporated hydride species and residual OH groups. A similar effect is also obtained by outgassing the catalyst at 773 K after each reduction treatment (curve b).

From this analysis, it is possible to differentiate two stages in the reduction of the support, which affect to different degrees the adsorption properties of the metal. In the range 373-673 K, incorporation of hydride species into the metal-support interface produces a significant decrease (63%) of hydrogen adsorption on the metal, which is recuperated by outgassing of the sample at 773 K. Above 673 K, these species are not stabilized in the support and the metal chemisorption loss must be related to other phenomena. In this case, the irreversible loss of hydrogen adsorption on the metal could be interpreted by blocking of adsorption sites with TiO_x species, as deduced from different techniques.[6-9,11,18,19,24] However, physical blocking of these sites does not explain why Δ decreases for outgassed samples, after reductions above 673 K (see dashed curve in Figure 2). For this, it is necessary to admit the presence of electronic interactions between the metal and TiO_x and/or reduced support. Moreover, the reduction of the support at high temperatures producing a significant elimination of oxygen atoms near metal particles points to the formation of rhodium-titanium bondings, not affected by outgassing treatments. In this way, the coverage of rhodium by TiO_x species should extend the metal-support interface, reinforcing our experimental observations. In summary, the NMR results reported in this work show the influence of the support reduction degree on the metal-support interaction. In particular, the incorporation of hydrogen and the formation of bondings in the metal-support interface explain the changes observed in the metal electronic properties for the two identified stages.

Acknowledgment. This research was supported by a grant from the Comisiôn Interministerial de Ciencia y Tecnología (CICYT). J.P.B. thanks the Ministerio de Educaciôn y Ciencia of Spain for a postgraduate fellowship.

Registry No. Rh, 7440-16-6; TiO_2, 13463-67-7; H_2, 1333-74-0.

{Bis(3-*tert*-butylpyrazolyl)hydroborato}zinc Alkyl Derivatives: Competitive Reactivity of Zn-C and B-H Bonds

Ian B. Gorrell, Adrian Looney, and Gerard Parkin*

Department of Chemistry, Columbia University New York, New York 10027

Arnold L. Rheingold

Department of Chemistry, University of Delaware Newark, Delaware 19716

Received February 16, 1990

We have recently described the syntheses and reactivity of the zinc[1] and magnesium[2] alkyl derivatives $\{\eta^3\text{-HB(3-Bu}^t\text{pz)}_3\}$MR (3-Bu^{t}pz = 3-$C_3N_2Bu^tH_2$; M = Zn, Mg; R = CH_3, CH_2CH_3), in which the tris(3-*tert*-butylpyrazolyl)hydroborato ligand provides a well-defined environment about the metal centers. Comparison of the reactivity of the Zn-C and Mg-C bonds in these complexes has provided good evidence for the intrinsic higher reactivity of the Mg-C vs the Zn-C bonds in isostructural derivatives. We were interested in investigating changes in reactivity at the metal center upon lowering the coordination number at the metal from 4 to 3. Here we describe the syntheses and reactivity of the three-coordinate monoalkyl zinc derivatives $\{\eta^2\text{-H}_2\text{B(3-Bu}^t\text{pz)}_2\}$ZnR (R = CH_3, CH_2CH_3, $C(CH_3)_3$).

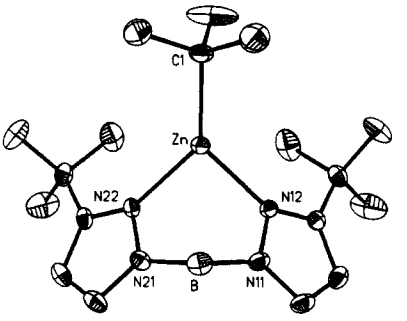

Figure 1. ORTEP diagram of $\{\eta^2\text{-B(3-Bu}^t\text{pz)}_2\}\text{ZnC(CH}_3)_3$. For clarity, thermal ellipsoids are shown at 20% probability. Selected bond distances (Å) and angles (deg): Zn-C(1) = 1.995 (7), Zn-N(12) = 2.040 (5), Zn-N(22) = 2.045 (6), N(11)-N(12) = 1.367 (8), N(21)-N(22) = 1.377 (8), B-N(11) = 1.547 (10), B-N(21) = 1.541 (12); N(12)-Zn-N(22) = 94.3 (2), N(11)-B-N(21) = 108.2 (6), C(1)-Zn-N(12) = 132.2 (3), C(1)-Zn-N(22) = 132.7 (3).

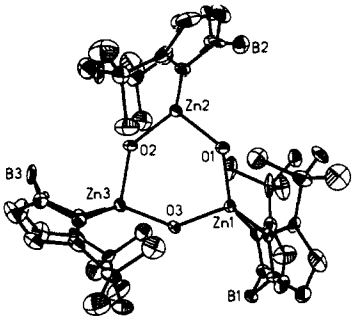

Figure 2. ORTEP diagram of $[\{\eta^2\text{-H}_2\text{B(3-Bu}^t\text{pz)}_2\}\text{Zn}(\mu\text{-OH})]_3$. For clarity, thermal ellipsoids are shown at 20% probability. Selected bond distances (Å) and angles (deg): Zn(1)-O(1) = 1.923 (8), Zn(1)-O(3) = 1.957 (10), Zn(2)-O(1) = 1.968 (9), Zn(2)-O(2) = 1.888 (9), Zn(3)-O(2) = 1.985 (8), Zn(3)-O(3) = 1.917 (10), Zn(1)-N(12) = 2.048 (9), Zn(1)-N(42) = 2.054 (11) Zn(2)-N(22) = 2.034 (10), Zn(2)-N(52) = 2.022 (11), Zn(3)-N(32) = 2.033 (11), Zn(3)-N(62) = 2.035 (11); O(1)-Zn(1)-O(3) = 103.6 (4), O(1)-Zn(2)-O(2) = 104.0 (4), O(2)-N(3)-O(3) = 102.0 (4), Zn(1)-O(1)-Zn(2) = 135.3 (5), Zn(2)-O(2)-Zn(3) = 137.2 (5), Zn(1)-O(3)-Zn(3) = 137.5 (4), N(12)-Zn(1)-N(42) = 94.3 (4), N(22)-Zn(2)-N(52) = 94.4 (4), N(32)-Zn(3)-N(62) = 93.4 (4).

Scheme I

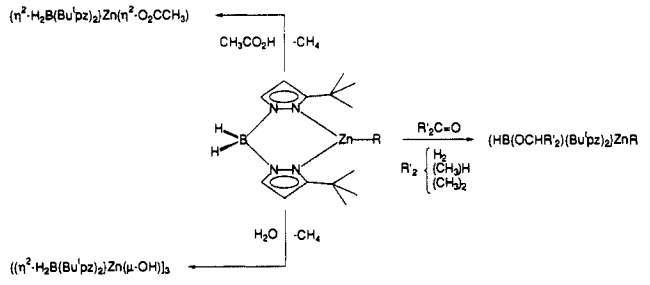

The zinc alkyl complexes $\{\eta^2\text{-H}_2\text{B(3-Bu}^t\text{pz)}_2\}$ZnR (R = CH_3, CH_2CH_3, $C(CH_3)_3$) are readily prepared by metathesis of R_2Zn with $Tl\{H_2B(3\text{-Bu}^t\text{pz})_2\}$ (eq 1). The molecular structure of the

$$R_2Zn \xrightarrow[THF]{Tl\{H_2B(3\text{-Bu}^t\text{pz})_2\}} \{\eta^2\text{-H}_2\text{B(3-Bu}^t\text{pz)}_2\}\text{ZnR} \qquad (1)$$

tert-butyl derivatives $\{\eta^2\text{-H}_2\text{B(3-Bu}^t\text{pz)}_2\}\text{ZnC(CH}_3)_3$ has been determined by an X-ray diffraction study (Figure 1), which shows that the molecule contains a distorted trigonal planar zinc center with bond angles N(12)-Zn-N(22) = 94.3 (2)°, N(12)-Zn-C(1) = 132.2 (3)°, and N(22)-Zn-C(1) = 132.7 (3)°.[3] The degree

(1) Gorrell, I. B.; Looney, A.; Parkin, G. *J. Chem. Soc., Chem. Commun.* **1990**, 220-222.

(2) Han, R.; Looney, A.; Parkin, G. *J. Am. Chem. Soc.* **1989**, *111*, 7276-7278.

(3) Crystal data for $\{\eta^2\text{-H}_2\text{B(3-Bu}^t\text{pz)}_2\}\text{ZnC(CH}_3)_3$: Monoclinic, $P2_1/n$ (No. 14), a = 14.912 (7) Å, b = 8.556 (2) Å, c = 18.482 (5) Å, β = 112.86 (3)°, V = 2173 (2) Å^3, Z = 4, ρ(calcd) = 1.17 g cm^{-3}, μ(Mo Kα) = 11.7 cm^{-1}, λ(Mo Kα) = 0.71073 Å (graphite monochromator); 4235 unique reflections with 3° < 2θ < 52° were collected, of which 1948 reflections with $F_o > 6\sigma(F_o)$ were used in refinement; R = 5.54%, R_w = 6.82%, GOF = 1.21.

0002-7863/90/1512-4068$02.50/0

of coplanarity around zinc is indicated by the sum of the three bond angles, which equals 359.2 (8)°. Three coordination is rare for zinc,[4] and $\{\eta^2\text{-}H_2B(3\text{-}Bu^tpz)_2\}ZnC(CH_3)_3$ represents the first structurally characterized monomeric organozinc complex that exhibits such coordination.

The reactivity of the complexes $(\{\eta^2\text{-}H_2B(3\text{-}Bu^tpz)_2\}ZnR$ is shown in Scheme I. Protic reagents (H_2O and CH_3CO_2H) react specifically at the Zn–C bond to give $[\{\eta^2\text{-}H_2B(3\text{-}Bu^tpz)_2\}ZnX]_n$ (X = OH, $\eta^2\text{-}O_2CCH_3$) and eliminate the alkane. The hydroxo complex $[\{\eta^2\text{-}H_2B(3\text{-}Bu^tpz)_2\}Zn(\mu\text{-}OH)]_3$ has been characterized as a cyclic trimer by an X-ray diffraction study (Figure 2), and the molecule possesses approximately C_3 symmetry, with each hydroxo group bridging to zinc centers.[5] Although the X-ray structure determination did not reveal the location of the hydroxo hydrogen atoms, convincing evidence for their presence is provided by the absorption at 3611 cm^{-1} that is assigned to ν_{O-H} on the basis of the shifts observed for the isotopomers $[\{\eta^2\text{-}HB(3\text{-}Bu^tpz)_2\}Zn(\mu\text{-}OD)]_3$ and $[\{\eta^2\text{-}HB(3\text{-}Bu^tpz)_2\}Zn(\mu\text{-}^{18}OH)]_3$. The hydroxo bridge between each pair of zinc centers is asymmetric, and the lengths of the Zn–O bonds alternate in a short-long fashion around the Zn_3O_3 ring. Thus, it appears that the short Zn(1)–O(1), Zn(2)–O(2), and Zn(3)–O(3) bonds (average $Zn\text{–}O_{short}$ = 1.909 (21) Å) more closely represent normal covalent interactions (i.e., Zn–O), with the longer Zn(1)–O(3), Zn(2)–O(1), and Zn(3)–O(2) bonds (average $Zn\text{–}O_{long}$ = 1.970 (13) Å) more closely representing dative covalent interactions (Zn ← O).[6,7]

These metathesis reactions are analogous to those of the four-coordinate complexes, $\{\eta^3\text{-}HB(3\text{-}Bu^tpz)_3\}ZnR$. However, whereas the tris(3-*tert*-butylpyrazolyl)hydroborato complexes $\{\eta^3\text{-}HB(3\text{-}Bu^tpz)_3\}ZnR$ only show reactivity at the Zn–C bond, the bis(3-*tert*-butylpyrazolyl)hydroborato derivatives also exhibit reactivity at an additional site, namely, the B–H bond. Thus, the bis(3-*tert*-butylpyrazolyl)hydroborato complexes $\{\eta^2\text{-}H_2B(3\text{-}Bu^tpz)_2\}ZnR$ (R = CH_3, CH_2CH_3) react with aldehydes and ketones, $(CH_2O)_n$, CH_3CHO, and $(CH_3)_2CO$, to give the derivatives $\{HB(OR')(3\text{-}Bu^tpz)_2\}ZnR$ (R′ = CH_3, CH_2CH_3, $CH(CH_3)_2$), as a result of insertion into the B–H bond. We have not yet determined whether the alkoxo substituents on boron are also coordinated to the zinc center, i.e., $\{\eta^2\text{-}HB(OR')(3\text{-}Bu^tpz)_2\}ZnR$ vs $\{\eta^3\text{-}HB(OR')(3\text{-}Bu^tpz)_2\}ZnR$. Although other bis(pyrazolyl)hydroborato metal complexes have also demonstrated the capability of reducing ketones to alcohols, functionalized bis(pyrazolyl)hydroborato products were not isolated.[8]

Thus, in conclusion, the bis(3-*tert*-butylpyrazolyl)hydroborato derivatives $\{\eta^2\text{-}H_2B(3\text{-}Bu^tpz)_2\}ZnR$ exhibit two different reactivity pathways. The Zn–C bonds are the sites of reactivity with protic reagents such as H_2O and CH_3CO_2H, and the B–H bonds are the preferred sites of reactivity for insertion with ketones and aldehydes.

Acknowledgment is made to the donors of the Petroleum Research Fund, administered by the American Chemical Society, for partial support of this research, and we thank Professor Arne Haaland for discussions.

Supplementary Material Available: Tables of spectroscopic data for all new compounds and tables of crystal and intensity collection data, atomic coordinates, bond distances and angles, and anisotropic displacement parameters and ORTEP drawings for $\{\eta^2\text{-}H_2B(3\text{-}Bu^tpz)_2\}ZnC(CH_3)_3$ and $[\{\eta^2\text{-}H_2B(3\text{-}Bu^tpz)_2\}Zn(\mu\text{-}OH)]_3$ (29 pages); tables of observed and calculated structure factors for $\{\eta^2\text{-}H_2B(3\text{-}Bu^tpz)_2\}ZnC(CH_3)_3$ and $[\{\eta^2\text{-}H_2B(3\text{-}Bu^tpz)_2\}Zn(\mu\text{-}OH)]_3$ (30 pages). Ordering information is given on any current masthead page.

(4) (a) Gruff, E. S.; Koch, S. A. *J. Am. Chem. Soc.* **1989**, *111*, 8762–8763. (b) Al-Juaid, S. S.; Buttrus, N. H.; Eaborn, C.; Hitchcock, P. B.; Roberts, A. T. L.; Smith, J. D. S.; Sullivan, A. C. *J. Chem. Soc., Chem. Commun.* **1986**, 908–909. (c) Bell, N. A.; Shearer, H. M. M.; Spencer, C. B. *Acta Crystallogr.* **1983**, *C39*, 1182–1185. (d) Petersen, R. B.; Ragosta, J. M.; Whitwell, G. E., II; Burlitch, J. M. *Inorg. Chem.* **1983**, *22*, 3407–3415. (e) Romanenko, V. D.; Shul'gin, V. F.; Skopenko, V. V.; Markovskii, L. N. *Zh. Obshch. Khim.* **1984**, *54*, 2791–2792.

(5) Crystal data for $[\{\eta^2\text{-}H_2B(3\text{-}Bu^tpz)_2\}Zn(\mu\text{-}OH)]_3$: Orthorhombic, $Pc2_1n$ (No. 33, nonstandard setting for $Pna2_1$), a = 12.302 (2) Å, b = 20.057 (6) Å, c = 22.110 (2) Å, V = 5455 (2) Å^3, Z = 4, ρ(Mo Kα) = 125 g cm^{-3}, μ(calcd) = 13.8 cm^{-1}, λ(Mo Kα) = 0.71073 Å (graphite monochromator); 4948 unique reflections with $3° < 2\theta < 50°$ were collected, of which 2946 reflections with $F_o > 5\sigma(F_o)$ were used in refinement; R = 7.72%, R_w = 6.37%, GOF = 1.20.

(6) The reference value for a pure single covalent Zn–O bond has been adopted to be 1.89 Å. Haaland, A. *Angew. Chem., Int. Ed. Engl.* **1989**, *28*, 992–1000.

(7) Other structurally characterized zinc hydroxo complexes include $[(Me_2PhSi)_3CZn(\mu\text{-}OH)]_2$ (1.899 (9) Å, ref 7a) and $[Zn_2(Bu^t_2P)_2(OH)(\mu\text{-}OH)]_2$ (2.30 (2) and 2.32 (2) Å, ref 7b). (a) Al-Juaid, S. S.; Buttrus, N. H.; Eaborn, C.; Hitchcock, P. B.; Roberts, A. T. L.; Smith, J. D. S.; Sullivan, A. C. *J. Chem. Soc., Chem. Commun.* **1986**, 908–909. (b) Arif, A. M.; Cowley, A. H.; Jones, R. A.; Koschmieder, S. U. *J. Chem. Soc., Chem. Commun.* **1987**, 1319–1320.

(8) Paolucci, G.; Cacchi, S.; Caglioti, L. *J. Chem. Soc., Perkin Trans. 1* **1979**, 1129–1131.

^{6}Li and ^{15}N Nuclear Magnetic Resonance Spectroscopic Studies of Lithiated Cyclohexanone Phenylimine Revisited. Aggregation-State Determination by Single-Frequency ^{15}N Decoupling

James H. Gilchrist, Aidan T. Harrison, David J. Fuller, and David B. Collum*

Department of Chemistry, Baker Laboratory Cornell University, Ithaca, New York 14853-1301

Received December 26, 1989

^{6}Li and ^{15}N NMR spectroscopy has proven to be a powerful probe of the atom connectivities and aggregation states of lithium dialkylamides and lithiated imines in solution.[1-4] Multiplicities consistent with monomers, cyclic oligomers, ion triplets, and mixed aggregates (Chart I; **1–4**) have all been recorded on substrates isotopically enriched in ^{6}Li and ^{15}N. The two major limitations of the double-labeling technique are as follows: (1) topologically equivalent cyclic oligomers—cyclic dimers, trimers, and tetramers—cannot be rigorously distinguished; and (2) the ^{15}N and ^{6}Li multiplets are not readily correlated when several chemically inequivalent sites are observed. We will demonstrate that ^{6}Li–^{15}N resonance correlations resulting from very simple single-frequency decoupling distinguishes cyclic dimers from higher oligomers for the lithiated phenylimine of cyclohexanone (**5**).[1,5]

^{6}Li and ^{15}N NMR spectroscopic studies of [^{6}Li,^{15}N]-**5** have been described previously; representative spectra are illustrated in Figure 1A,B.[1] The two ^{6}Li 1:2:1 triplets ($J_{N\text{-}Li}$ = 3–4 Hz each) and the two 1:2:3:2:1 ^{15}N quintets ($J_{N\text{-}Li}$ = 3–4 Hz) appear to derive from cyclic aggregate structural units. The 2:1 ratio of aggregate-derived resonances remains constant with changes in the concentration of either **5** or THF (using toluene-d_8 as diluent).[6] The two ^{6}Li triplets and two ^{15}N quintets are consistent with either a mixture of stereoisomeric cyclic dimers **6** and **7** or cis,trans trimer **8** (*Cy* = 1-cyclohexenyl). Colligative measurements,[7] crystallographic analogies,[7] the absence of resonances expected for the all-cis stereoisomeric trimer **9**, and ab initio calculations on $(H_2NLi\cdot S)_n$ oligomers[8] all implicate dimers **6** and **7**. Nevertheless,

(1) Kallman, N.; Collum, D. B. *J. Am. Chem. Soc.* **1987**, *109*, 7466. Wanat, R. A.; Collum, D. B.; Van Duyne, G.; Clardy, J.; DePue, R. T. *J. Am. Chem. Soc.* **1986**, *108*, 3416.

(2) Galiano-Roth, A. S.; Michaelides, E. M.; Collum, D. B. *J. Am. Chem. Soc.* **1988**, *110*, 2658.

(3) Jackman, L. M.; Scarmoutzos, L. M.; Porter, W. *J. Am. Chem. Soc.* **1987**, *109*, 6524. Jackman, L. M.; Scarmoutzos, L. M. *J. Am. Chem. Soc.* **1987**, *109*, 5348. Jackman, L. M.; Scarmoutzos, L. M.; Smith, B. D.; Williard, P. G. *J. Am. Chem. Soc.* **1987**, *109*, 6058.

(4) Depue, J. S.; Collum, D. B. *J. Am. Chem. Soc.* **1988**, *109*, 5518. Galiano-Roth, A. S.; Collum, D. B. *J. Am. Chem. Soc.* **1989**, *111*, 6772.

(5) Determination of ^{13}C–^{6}Li correlations in alkyllithiums using two-dimensional techniques, as well as use of a ^{2}H lock channel to observe lithium, have been reviewed. Günther, H.; Moskau, D.; Bast, P.; Schmalz, D. *Angew. Chem., Int. Ed. Engl.* **1987**, *26*, 1212.

(6) At substantially elevated THF concentrations, the aggregate resonances are replaced by a ^{6}Li doublet ($J_{N\text{-}Li}$ = 6.3 Hz) and the 1:1:1 ^{15}N triplet ($J_{N\text{-}Li}$ = 6.1 Hz) fully characteristic of a monomer.[1]

(7) See ref 2 for leading references.

(8) Armstrong, D. R.; Mulvey, R. E.; Walker, G. T.; Barr, D.; Snaith, R.; Clegg, W.; Reed, D. *J. Chem. Soc., Dalton Trans.* **1987**, 617.

0002-7863/90/1512-4069$02.50/0